

# Microseismic monitoring of Vaca Muerta completions in the Neuquén Basin, Argentina

David Curia<sup>1</sup>, Peter M. Duncan<sup>2</sup>, Michael Grealy<sup>2</sup>, Jon McKenna<sup>2</sup>, and Andrew Hill<sup>2</sup>

## Abstract

The Vaca Muerta shale oil play in Argentina's Neuquén Basin is expected to make a large contribution to Argentina's hydrocarbon production in the future. In 2013, the U.S. Energy Information Administration estimated that the Vaca Muerta had technically recoverable reserves of 308 Tcf gas and 16 billion bbl of oil and condensate, making it the third largest shale oil reservoir in the world at that time. Wintershall Energia has been active in the Neuquén Basin since 1994. In 2014, it acquired a controlling interest in the Aguada Federal block with an intention to exploit the Vaca Muerta oil shale occurrence within that block. At the outset of its development program, Wintershall decided to incorporate microseismic monitoring to help understand completions in the Vaca Muerta. Monitoring of the completion of vertical well AF.x-1 was accomplished with a surface array. The goal of the monitoring was to inform later decisions on horizontal wellbore direction, wellbore and stage spacing, and landing depth. Results of the surface array monitoring were also used in the design of a permanent buried array intended to monitor subsequent development wells. The buried array was installed in September 2016 and consists of 126 stations spread at an interval distance of approximately 500 m over an area of roughly 5 by 7 km. Each station has geophones placed over a depth range of 20 to 50 m subsurface. The first two horizontal development wells in the project, AF.x-4h and AF.x-9h, were completed in late December 2016 and early January 2017. The second set of two wells, AF.x-3h and AF.x-7h, was completed from May to June 2017. The 4h and the 7h were landed in the upper Middle Vaca Muerta while the 9h and 3h were drilled about 100 m deeper, landing still in the Middle Vaca Muerta. The lateral length of each well was approximately 1000 m, and each was completed with 11 plug-and-perf stages. Stage length and interval were varied along the wells to test various completion strategies. The completions of all four wells were successfully monitored using the buried array. These microseismic data provide a detailed description of the fracture network created by the treatments. Focal mechanisms determined for the detected events have been used to understand the stress distribution in the reservoir and to further refine the completion parameters for future development wells.

## Introduction

Oil and gas production in Argentina dates back to the early 1900s after oil was discovered in 1907 near the city of Comodoro Rivadavia, Chubut. In 2016, Argentina produced an average of 693,000 b/d of petroleum and other liquids (U.S. Energy Information Administration [EIA], 2017) making it the world's 26<sup>th</sup> largest producer. The Vaca Muerta shale oil play in Argentina's Neuquén Basin is expected to play an important role in future

production. In 2013, the EIA (EIA, 2013) estimated that the Vaca Muerta had technically recoverable reserves of 308 Tcf gas and 16 billion bbl of oil and condensate making it the third largest shale oil reservoir in the world at that time.

The Vaca Muerta is an Upper Jurassic to Lower Cretaceous marine shale located in the Neuquén Basin on the eastern side of the Andes in west-central Argentina (Figure 1). The formation outcrops on the edges of the basin and reaches depths of approximately 2830 m in the basin center with thicknesses ranging from 63 to 535 m. The prospective area, including the oil-rich, condensate-rich, and dry gas zones, is estimated to cover about 30,000 km<sup>2</sup> (EIA, 2013).

Wintershall began its oil and gas activities in Argentina more than 35 years ago and is the fourth largest producer. Wintershall currently has an interest in 15 oil and gas fields in the country and produces about 26 million BOE annually. Wintershall has been active in the Neuquén Basin since 1994. In 2014, it acquired



Figure 1. Map showing the hydrocarbon-producing basins of Argentina with the location of the Neuquén Basin noted.

<sup>1</sup>Wintershall Energia S.A.

<sup>2</sup>MicroSeismic Inc.

<https://doi.org/10.1190/tle37040262.1>

a controlling interest in the Aguada Federal block with an intention to exploit the Vaca Muerta oil shale occurrence there.

In this article, we discuss the application of microseismic monitoring of both vertical and horizontal wells in the early phases of exploration and development of this play. In particular, we discuss the steps that led to placing a permanent life-of-field monitoring array in the field, the results of monitoring, and some of the initial conclusions drawn from the data.

### Early-stage field development

Wintershall's development program for the Aguada Federal block (Figure 2) has been planned in four principal project phases: (1) a technology phase to reduce geologic uncertainty, prove hydrocarbon flow from the reservoir, and assess the resource with widely spaced test wells; (2) a pilot phase to reduce production uncertainty and to test well productivity and effectiveness of hydraulic fracture well stimulation applied to multiwell pads with closely spaced horizontal wells on predefined, small acreages; (3) a predevelopment phase to reduce economic uncertainty and demonstrate the project commerciality by continually reducing costs and increasing well productivity; and (4) a development phase in which infill wells are completed in a manufacturing style mode designed to deplete the resource.

During the technical phase, Wintershall elected to monitor the stimulation of the AF.x-1 vertical well as part of the play assessment. The well was stimulated in August 2015 in four stages, penetrating the Upper, Middle, and Lower Vaca Muerta. Monitoring was performed with a surface FracStar array as depicted in Figure 3. The results were sufficiently compelling that Wintershall continued with microseismic monitoring into the technical phase of development. The completions of four horizontal wells, located on the same pad as the AF.x-1, were monitored from December 2016 through June 2017. Monitoring of these wells was achieved with a permanent buried array as pictured in Figure 3.

### Microseismic monitoring well AF.x-1

Microseismic monitoring is a vital part of shale exploration and development workflows. In fact, in the prolific Permian Basin of Texas, seven of the top 10 operators on the Midland side have integrated microseismic into their technology portfolio as have five of the top 10 operators in the Delaware portion. (Per Drillinginfo.com. Top operators are defined as highest average peak BOEPD by basin. Data for seven out of 10 in the Midland Basin is for the period February 2016 through February 2017; five out of 10 in the Delaware Basin covers February 2014 to February 2017.)

By locating the hypocenters of the seismic signals propagating from induced fractures or reactivated natural fractures and through

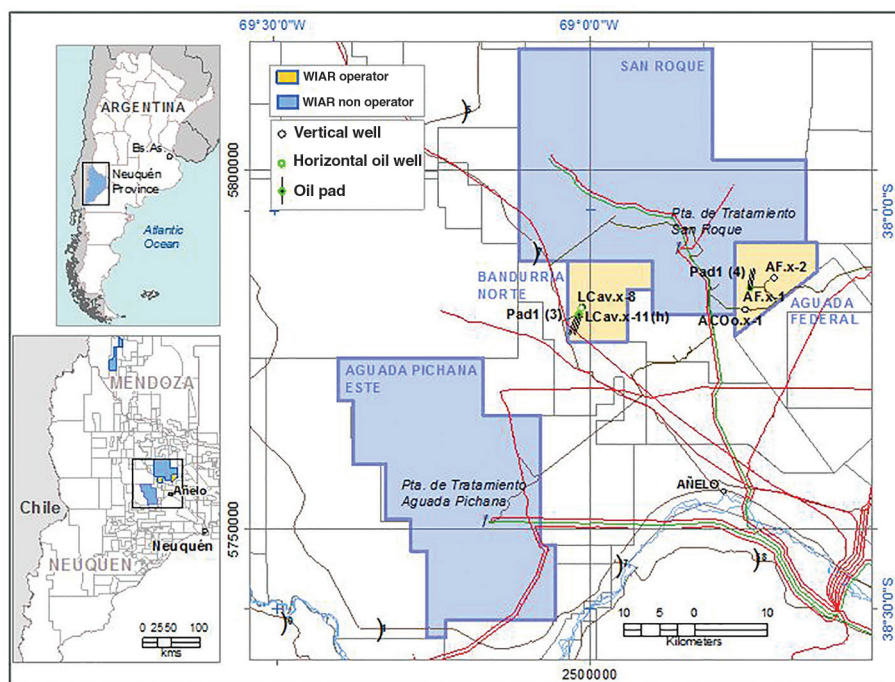


Figure 2. Wintershall (WIAR) blocks in the Neuquén Basin.

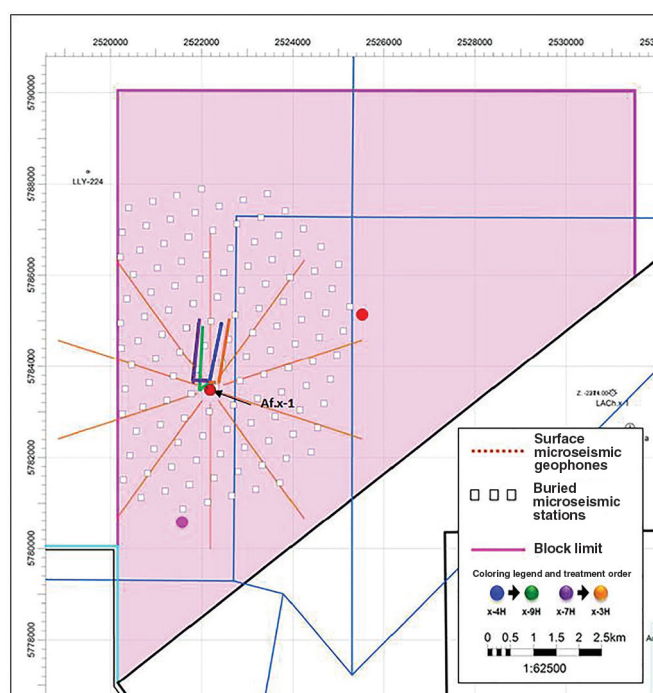


Figure 3. Location map of the stimulated wells and monitoring arrays in the Aguada Federal block. Surface and microseismic buried array locations are shown as orange lines and white squares, respectively. The vertical AF.x-1 well is located at the indicated red circle. The four horizontal wells are labeled by their color.

more in-depth analysis of the nature of these seismic events, it is possible to develop a rich understanding of the geometry of the permeability-enhanced volume created by stimulation of the well. The results of these analyses can be used to help optimize well placement and stimulation programs in unconventional reservoirs (Maxwell, 2010). After considering the success of this technology

in other plays, Wintershall decided to incorporate microseismic monitoring into its development of the Vaca Muerta.

The completion of well AF.x-1 was monitored with a surface array consisting of 10 lines, approximately 3 km long and of 214 channels each, placed symmetrically around the well's surface location as pictured in Figure 3. The station interval was 14 m. There were 12 geophones (conventional 10 Hz, vertical) in each group, spaced evenly between the stations along the radial arms of the array. The vertical well was treated in four stages over the depth range of 2642 to 2841 m, covering the Lower, Middle, and Upper Vaca Muerta intervals. The goal of the monitoring was to inform later decisions on horizontal wellbore direction, wellbore and stage spacing, and landing depth.

A surface array was selected for the monitoring for several reasons. Available monitor wells were too far removed from the location of AF.x-1 to be of practical use. Wintershall was interested in determining moment tensors, failure mechanisms, and stress distribution in the reservoir. Each of these goals was made more feasible with a large-aperture, wide-azimuth surface array (Duncan and Eisner, 2010). In addition, Wintershall was interested in establishing a life-of-field permanent monitoring array over the block at some point in the development cycle. Such a permanent array incurs front-end costs for installation, but it then can be used for the monitoring of many wells over the life of the field, thereby reducing unit monitoring costs substantially while achieving the same monitoring objectives as a large surface array. Beyond frac mapping, monitoring a large number of wells in a developing field is beneficial for detecting production-related seismicity, directly mapping individual well drainage volumes, and determining the "interconnectivity" of individual wells. Monitoring the completions of a large number of wells under such a permanent array can generate improvements in the accuracy of both hydraulic stimulation design and reservoir simulation models. One goal of the AF.x-1 surface array monitoring was to develop design parameters for such a permanent array.

The observations derived from the microseismic monitoring of the AF.x-1 treatment were as follows:

- The surface array was successful at detecting event magnitudes in the range of -0.7 to -2.8 with a magnitude of completeness around -1.8.
- The majority of events occurred in two clusters, one in the Upper Vaca Muerta and one in the overlying Quintuco.
- Few events were detected in association with the treatment of the Lower Vaca Muerta. There are several possible explanations for this observation. First, the treatment volume pumped into the lower stage was one-third of that pumped into the upper. Second, the Upper Vaca Muerta and Quintuco are known to have greater Young's and shear moduli, which suggests they would fail with a more "brittle" behavior. It is possible that the Lower Vaca Muerta, being more ductile, merely failed without microseismic emissions in the magnitude range detected with the surface array. Third, it is our experience that the first stage pumped into a reservoir often will produce fewer detected microseismic events. We believe this observation may be ascribed to the fact that the reservoir is not yet "pressured up" at that point.

Finally, some authors (for example, Osorio and Muzzio, 2013) have reported that stress anisotropy is higher in the Upper Vaca Muerta than it is in the Lower, suggesting another cause for the different response.

- Three focal mechanisms were resolved. The dominant mechanism in the Upper Vaca Muerta was oblique slip on a vertical plane striking at 90°. The dominant mechanism for the events occurring in the overlying Quintuco was reverse oblique on a 75° dipping plane striking at 35°. The third mechanism observed was a vertical strike-slip set of fractures mostly occurring distal to the well with a strike of 50°.
- Most events have dominantly double-couple, nonvolumetric source mechanisms. Of the volumetric changes that do occur, more events are apparently closing events, rather than opening. This is interpreted to mean that the microseismic events represent the interaction between hydraulic fractures propagating parallel to the direction of maximum horizontal stress ( $S_{Hmax}$ ) and preexisting natural fractures. Microseismic events originate where the induced fractures intersect natural fractures that are well oriented with respect to  $S_{Hmax}$ .
- The  $S_{Hmax}$  orientation, as revealed by event source mechanisms, is approximately east to west.
- Taking into account the half-length of the microseismic cloud, the indicated wellbore spacing is 150 m.
- Taking into account the longitudinal width of the microseismic zone, the indicated stage spacing is 75 m.
- The recommended wellbore orientation is ~N10°E based on both the direction of event propagation and the estimate of  $S_{Hmax}$  azimuth from the observed focal mechanisms.
- The recommended landing zone, based on the observed fracturing behavior, is the Upper Vaca Muerta.

### Permanent array design

Given the success with monitoring the AF.x-1 using a surface array, Wintershall proceeded with the design and installation of a permanent, near-surface buried array for the project's pilot phase. The important design considerations for the establishment of such a buried microseismic array are as follows:

- depth of geophone placement
- individual station array configuration
- areal extent of the array (aperture)
- number of stations (fold)

Paramount to all of these decisions is the ambient surface noise level and some knowledge of how that noise falls off with depth (Duncan and Eisner, 2013). The monitoring of AF.x-1 already had provided a measurement of the ambient noise at the surface and the event magnitudes that might be expected during the treatment of the next wells. To measure the falloff of the noise with depth, a 130 m deep well was drilled and loaded with a vertical wireline array consisting of 10 geophones spaced 10 m apart. Ambient noise was recorded over a 72-hour period. The observed attenuation of ambient noise with depth is presented in Figure 4. The root-mean-square (rms) noise at the surface had a median value of 50 nm/s. The noise was observed to fall off 33 dB in the first 40 m and then 26 dB in the next 80 m.



Knowing the ambient noise falloff with depth, one can proceed to the next step in the design process. There is a design tradeoff between the number of stations (fold) and the depth of each station. The driver behind this tradeoff is the acceptable noise level for a given target signal level. Signal-to-noise ratio (S/N) is key to the uncertainty in location and focal mechanism estimates for each and every event (Thornton, 2012; Mueller et al., 2013). S/N determines the effective floor in the detection level of the array. Drilling deeper reduces the ambient noise at the receiver (higher S/N) but increases drilling charges. Designing for more stations (higher fold) results in a net gain in S/N through the reduction of random noise but at the expense of drilling more holes, needing more equipment in the field, and having more traces to process.

The approach taken in the Wintershall array design was to model the array response using a target magnitude of completeness of  $-2.0$  and a target S/N of 3:1. The falloff of signal with distance

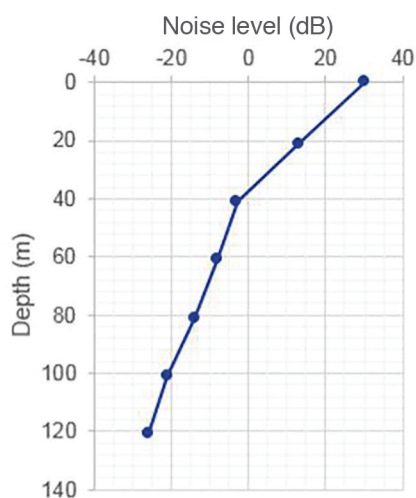


Figure 4. Noise test results showing noise reduction with depth.

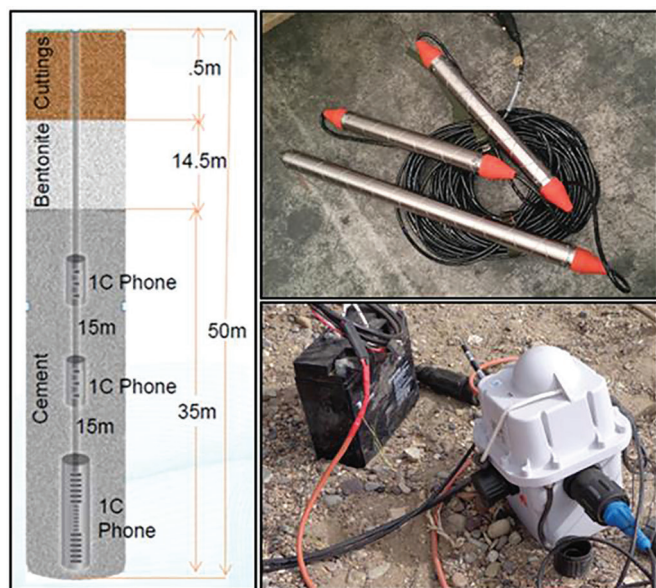


Figure 5. Sketch of a buried array installation along with pictures of the sondes and the wireless recorder.

was estimated using a  $Q$  of 40, the value of which was obtained from vertical seismic profile work carried out in the area. With appropriate consideration of cost-benefit tradeoffs, the final design of the array called for 126 stations spread at an interval distance of approximately 500 m over a roughly 5 by 7 km grid as displayed in Figure 3. Each station consisted of three geophone pods cemented at depths of 50, 35, and 20 m below surface resulting in 368 seismic channels recorded at a 2 ms sampling. Each pod consisted of six 4.5 Hz single-component vertical geophones wired in series (Figures 5 and 6).

### Microseismic monitoring wells AF.x-4h, AF.x-9h, AF.x-3h, and AF.x-7h

The first wells of the pilot phase, the AF.x-4h and AF.x-9h, were completed in late December 2016 and early January 2017. The second set of two wells, the AF.x-3h and AF.x-7h, was completed from May to June 2017. The 4h and 7h were landed in the upper Middle Vaca Muerta while the 9h and 3h were drilled about 100 m deeper, landing still in the Middle Vaca Muerta. The lateral length of each well was approximately 1000 m, and each was completed with 11 plug-and-perf stages. Stage length and interval were varied along the wells to test the reservoir's response to various completion design parameters.

The rms ambient noise observed on the buried array over the 103 hours of recording was observed to be about 5 nm/s. This is a full order of magnitude below the ambient noise observed on the surface array. The hypocenters of the final event set are displayed in Figure 7. During this monitoring campaign, more seismic energy was recovered from deeper in the Vaca Muerta, likely as a result of the increased pumping effort from the multiple stages in the horizontal wells and the increased sensitivity of the buried array (Figure 8). Estimated uncertainty in the event locations as a function of S/N achieved with the buried array is plotted in Figure 9 (Thornton, 2012; Mueller et al., 2013).

Full moment tensor inversion (Aki and Richards, 1980) and focal mechanism determination were applied to all events with a S/N of 5 or greater (postprocessing). This resulted in 3994 distinct mechanism determinations. The three dominant



Figure 6. Installing the buried array in September 2016.

mechanisms are an approximately vertical dip-slip mechanism striking at 90° and two sets of strike-slip fractures, one striking at 150° and the other at 0°. A fourth mechanism, strike-slip at 50°, as was seen during the treatment of AF.x-1, was also present in small numbers. These mechanisms are consistent with published studies for the basin. For example, Garcia et al. (2013) report that the stress regime in the Neuquén changes from dominantly “normal” to dominantly “strike-slip” as one moves from east to west through the basin. The Aguada Federal block is in the intermediate or mixed zone. Bishop (2015) in work based on wellbore breakout studies, reports that  $S_{Hmax}$  in the area strikes east to west while the minimum horizontal stress ( $S_{hmin}$ ) strikes north to south. Bishop also reports conductive natural fractures at 50° and 155°.

A discrete fracture network (DFN) was constructed from the microseismic event catalog to create a more geologically reasonable

model of the fracture network activated by treatment of the wells. Each event hypocenter, as represented by a sphere in Figure 7, is replaced with a planar fracture element oriented with strike and dip equal to the strike and dip of the focal mechanism estimated for that particular event (Williams-Stroud and Eisner, 2014). The area of the planar fracture element is calculated from the moment magnitude of the particular event. Figure 10 displays a map and depth section view of the DFN derived from the microseismic monitoring of the four horizontal wells being discussed here.

The next step to be taken in the analysis and interpretation of these data is to upscale this fracture model into a stimulated reservoir volume (SRV) that maps the permeability enhancement of the reservoir achieved by the stimulation. Such a volume will be used as input to a conventional reservoir simulation to predict production volumes and pressure drawdown distributions for these wells over time (Shojaei and Lipp, 2016) with the caveat

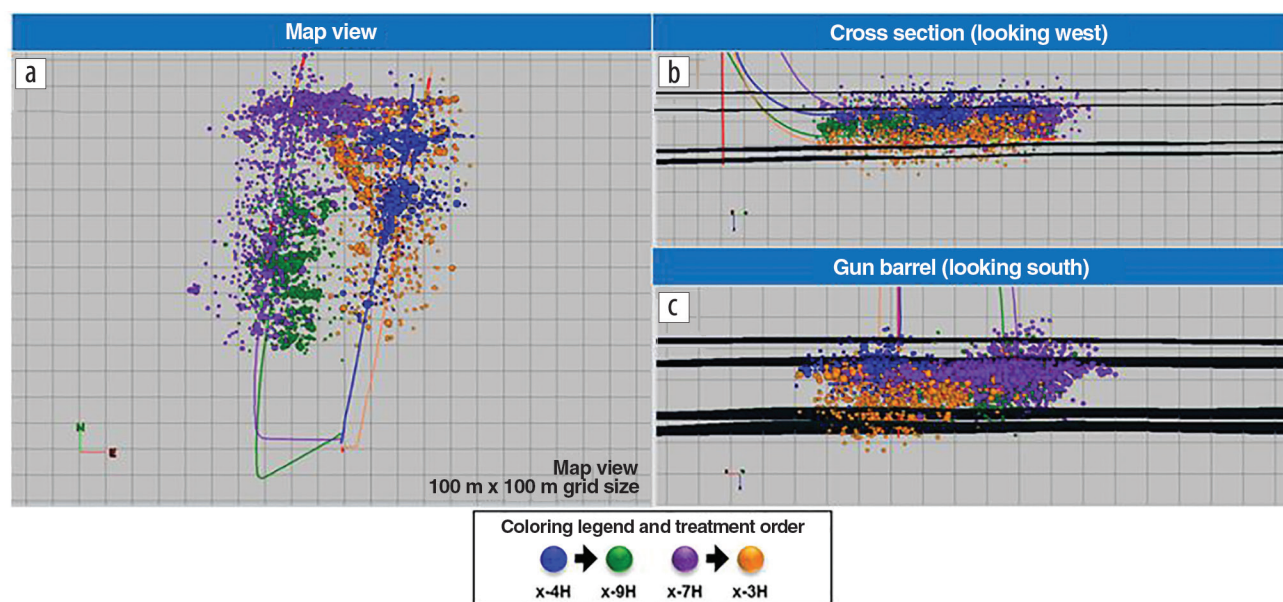


**Figure 7.** Hypocenter locations for the final event set captured during the treatment of the four horizontal wells. (a) Map view. (b) Depth view looking west. (c) Gun barrel view looking south. Horizon tops are shown for Upper, Middle, and Lower Vaca Muerta as well as the underlying Tordillo. Grid size in all plots is 100 × 100 m. Events are sized by magnitude.

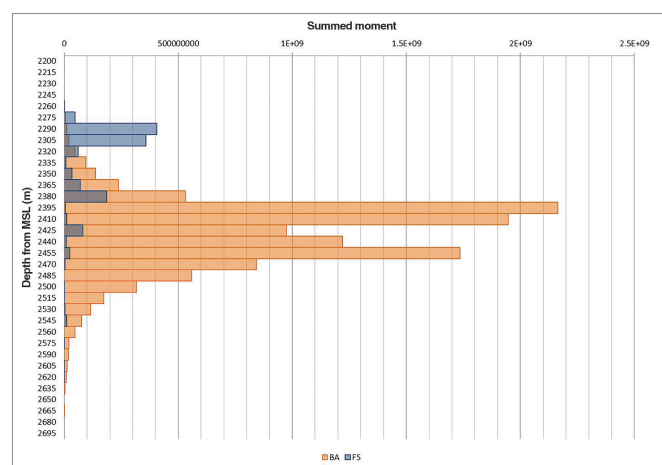


**Figure 8.** Cumulative seismic moment observed for the five Aguada Federal wells. Note the increased depth sensitivity with the buried array (orange) versus the surface FracStar (blue).

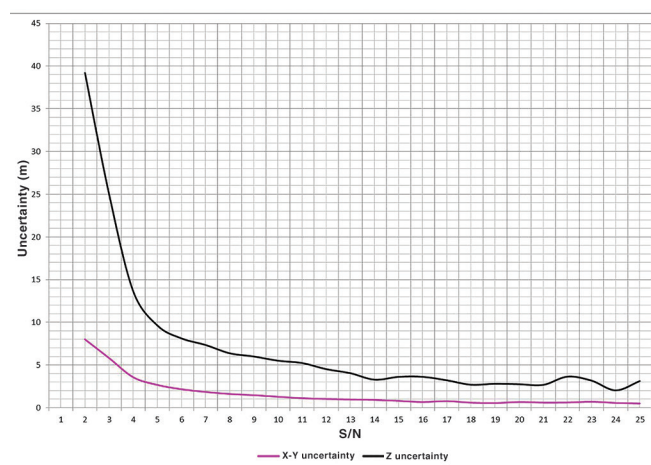


**Figure 9.** Horizontal (XY) and vertical (Z) estimated event location uncertainty as a function of S/N during the monitoring of wells AF.x-4h, 9h, 3h, and 7h using the buried array.



that allowance must be made for the extent to which the SRV actually received proppant filling.

### $S_{Hmax}$ and geomechanics

Another important extension of the focal mechanism determination is to use the distribution of observed fault motions to estimate the direction of  $S_{Hmax}$  and the ratio of principle stresses  $\phi$  at each point of failure as defined in equation 1:

$$\phi = \frac{(\sigma_2 - \sigma_3)}{(\sigma_1 - \sigma_3)}, \quad (1)$$

where  $\sigma_1$ ,  $\sigma_2$ , and  $\sigma_3$  are the three principal stresses (Michael, 1984; Angelier, 1989).

The estimate of this ratio is made under the assumption that the fracture slip is in the same direction as the resolved shear stress on the fracture plane (Bott, 1959). Assuming that one of the principal stresses is vertical and can be estimated from the

density log or other means, and that  $S_{hmin}$  can be estimated from a DFIT or similar test, then the direction and value of  $S_{Hmax}$  may be calculated for every microseismic event for which a mechanism is determined (Agharazi, 2016).

Applying this analysis to the monitoring results of horizontal wells, we can plot all the events on a Mohr's circle diagram as given in Figure 11. As the hydraulic fracture stimulation proceeds, the injected fluids act to increase the pore or fracture pressure in the reservoir, thereby reducing the net normal confining pressure until the ratio of shear stress to net normal stress exceeds the strength of the rock or the friction on a planar fracture. Fractures close to this condition are referred to as critically stressed. One can think of the hydraulic fracturing process as moving the circular figure in the plot below to the left relative to the axes, with failure occurring whenever the point representing the failure plane crosses the line of friction (Jaeger et al., 2008).

Each of the points on the plot in Figure 11 represents an observed microseismic event from the monitoring of the four horizontal completions. Hence, each event represents a failure of the rock. Points farther to the right are harder to fracture as highlighted by the color bands. Events plotting in the colder colors required a higher pore pressure to be present before failure occurred.

A practical application of this observation is that the Quintuco events activated in the treatment of AF.x-1 plot much farther to the right than do the events in the Vaca Muerta. In other words, the failure planes excited in the Quintuco Formation during treatment are less favorably oriented with respect to the principal stresses than are those observed to fail

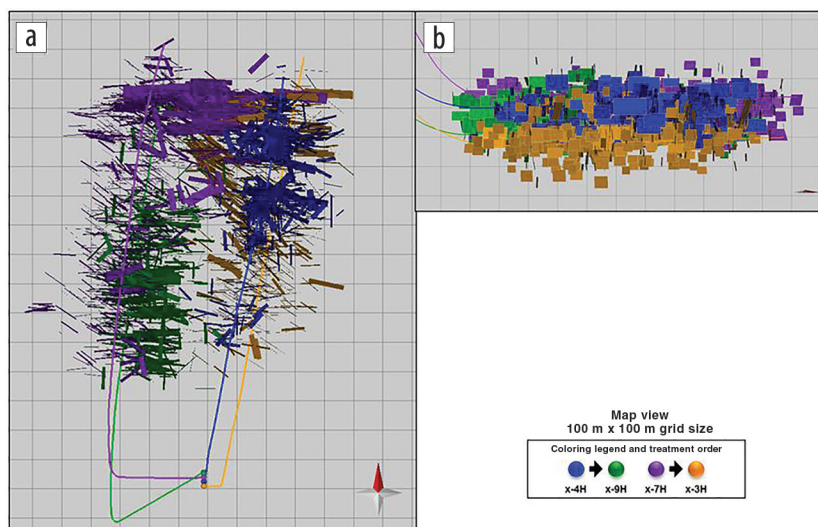


**Figure 10.** DFN derived from data displayed in Figure 9 using strike, dip and magnitude of the observed microseismic events. (a) Map view. (b) Depth view looking west. Grid size is 100 × 100 m.

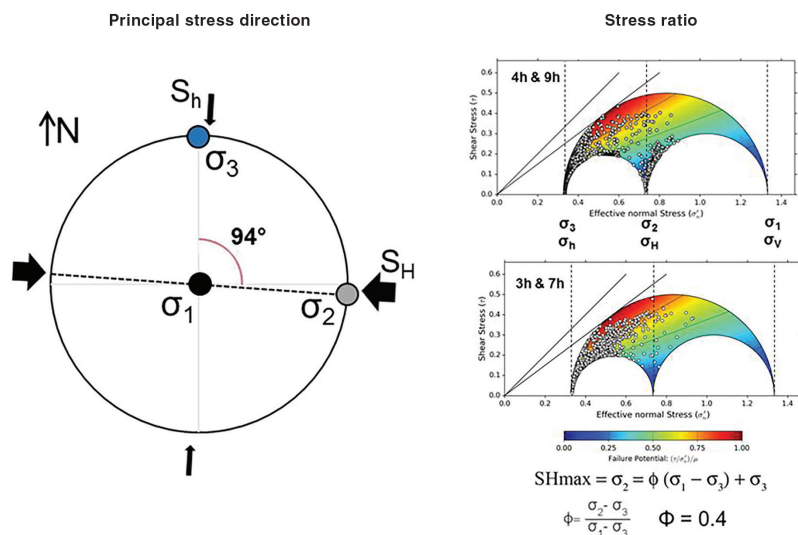


**Figure 11.** Geomechanical analysis results for the microseismic events captured during the treatment of the horizontal wells. The diagram on the left illustrates the directions determined for the three principal stresses on a lower hemisphere polar projection. The Mohr's circle plots on the right illustrate the relative magnitude of the stresses at the time of failure. The horizontal axis is the net stress acting normal to the event failure plane, and the vertical axis is the resultant shear stress on the fracture plane. The relative sizes of the principal stresses are shown by their position on the horizontal axis. The dots represent the position of the observed event fracture planes in this stress coordinate system. The straight lines represent hypothetical lines of friction, the ratio of shear stress to normal stress at which failure occurs. The colors indicate the state of stress at any point in this system with colder colors representing more stable or less likely to fail conditions. The equations illustrate how the value of  $S_{Hmax}$  is derived in a normal faulting regime once the stress ratio  $\phi$  has been estimated from the focal mechanisms.

in the Vaca Muerta Formation. Very few Quintuco events were observed in the treatment of the subsequent four horizontal wells, suggesting that during these treatments fluids penetrating to the Quintuco did not raise the pore pressure high enough to cause failure. Furthermore, the distribution of event orientations and their relative distance from failure or criticality observed while treating the horizontal wells suggest an opportunity to be selective and efficient when pumping. It would seem logical and economical to limit raising the pore pressure to the point where events oriented perpendicular to  $S_{Hmax}$  are triggered because they will tend to close first and make a minimal contribution to long-term production.

## Conclusion

Microseismic monitoring of the AF.x-1, AF.x-4h, AF.x-9h, AF.x-3h, and AF.x-7h was successful in helping Wintershall better understand and design an optimal completion strategy for the Vaca Muerta play, Neuquén Basin, Argentina. During the technical phase, the monitoring of a single vertical well with a large surface array established that a surface array could indeed detect events originating in the Vaca Muerta. The results provided insight on preferred horizontal well orientation, spacing, and landing zone. The data also helped establish the feasibility of a permanent life-of-field array that was later installed during the pilot phase of field development. A large-scale, permanent array was desired not only for the technical advantages provided by a large-aperture, wide-azimuth observation of the microseismic signals, but also for the technical and budgetary advantages of a permanent facility that would allow for the monitoring of multiple wells at a reasonable cost.

The permanent array of 128 stations was installed in late 2016. To date, the stimulations of four horizontal wells have been monitored with this array. These observations provide a detailed description of the fracture network created by the treatments. Focal mechanisms estimated for the detected events have been used to understand the stress distribution in the reservoir and to further refine the completion parameters for future wells. ■■

Corresponding author: pduncan@microseismic.com

## References

- Agharazi, A., 2016, Determination of maximum horizontal field stress from microseismic focal mechanisms — A deterministic approach: 50<sup>th</sup> U.S. Rock Mechanics/Geomechanics Symposium, ARMA, paper ARMA-2016-691.
- Aki, K., and P. G. Richards, 1980, *Quantitative seismology: Theory and methods*: W. H. Freeman and Co.
- Angelier, J., 1989, From orientation to magnitudes in paleostress determinations using fault slip data: *Journal of Structural Geology*, **11**, no. 1–2, 37–50, [https://doi.org/10.1016/0191-8141\(89\)90034-5](https://doi.org/10.1016/0191-8141(89)90034-5).
- Bishop, K., 2015, Mechanical stratigraphy of the Vaca Muerta Formation, Neuquén Basin, Argentina: M.S. thesis, Colorado School of Mines.
- Bott, M. H. P., 1959, The mechanics of oblique slip faulting: *Geological Magazine*, **96**, no. 2, 109–117, <https://doi.org/10.1017/S0016756800059987>.
- Duncan, P. M., P. G. Smith, K. Smith, W. B. Barker, S. Williams-Stroud, and L. Eisner, 2013, Microseismic monitoring in Early Haynesville development, in U. Hammes and J. Gale, eds., *Geology of the Haynesville gas shale in East Texas and West Louisiana*, U.S.A.: AAPG Memoir 105, 219–236.
- Duncan, P. M., and L. Eisner, 2010, Reservoir characterization using surface microseismic monitoring: *Geophysics*, **75**, no. 5, 75A139–75A146, <https://doi.org/10.1190/1.3467760>.
- EIA, 2017, International energy statistics, total petroleum and other liquids: US Energy Information Administration, US Department of Energy, <https://www.eia.gov/beta/international/data/browser>, accessed 27 February 2018.
- EIA, 2013, Technically recoverable shale oil and shale gas resources: An assessment of 137 shale formations in 41 countries outside the United States: US Energy Information Administration, US Department of Energy, [https://www.eia.gov/analysis/studies/worldshalegas/archive/2013/pdf/fullreport\\_2013.pdf](https://www.eia.gov/analysis/studies/worldshalegas/archive/2013/pdf/fullreport_2013.pdf), accessed 27 February 2018.
- Garcia, M. N., F. Sorenson, J. C. Bonapace, F. Motta, C. Bajuk, and H. Stockman, 2013, Vaca Muerta shale reservoir characterization and description: The starting point for development of a shale play with very good possibilities for a successful project: Unconventional Resources Technology Conference, <https://doi.org/10.1190/urtec2013-090>.
- Jaeger, J. C., N. G. W. Cook, and R. W. Zimmerman, 2008, *Fundamentals of rock mechanics*, 4<sup>th</sup> ed.: Blackwell Publishing.
- Maxwell, S., 2010, Microseismic: Growth born from success: *The Leading Edge*, **29**, no. 3, 338–343, <https://doi.org/10.1190/1.3353732>.
- Michael, A. J., 1984, Determination of stress from slip data: Faults and folds: *Journal of Geophysical Research*, **89**, no. B13, 11,517–11,526, <https://doi.org/10.1029/JB089iB13p11517>.
- Mueller, M., M. Thornton, and L. Eisner, 2013, Uncertainty in surface microseismic monitoring: AAPG Search and Discovery article #41258.
- Osorio, J. G., and M. E. Muzzio, 2013, Correlation between microseismicity and geomechanics factors affecting the hydraulic fracturing performance in unconventional reservoirs — A field case in Neuquén: 47<sup>th</sup> U.S. Rock Mechanics/Geomechanics Symposium, ARMA, paper ARMA-2013-526.
- Shojaei, H., and C. Lipp, 2016, Optimizing unconventional field development through an integrated reservoir characterization and simulation approach: Unconventional Resources Technology Conference, URTEC-2435418-MS.
- Thornton, M., 2012, Resolution and location uncertainties in surface microseismic monitoring: GeoConvention.
- Williams-Stroud, S. C., and L. Eisner, 2014, Method for determining discrete fracture networks from passive seismic signals and its application to subsurface reservoir simulation: U.S. Patent 8,902,710 B2.